

## University of Wollongong Research Online

---

Faculty of Engineering - Papers (Archive)

Faculty of Engineering and Information  
Sciences

---

2009

### Thermal-strain-induced enhancement of electromagnetic properties of SiC-MgB2 composites

Rong Zeng

*University of Wollongong, rzeng@uow.edu.au*

S X. Dou

*University of Wollongong, shi@uow.edu.au*

Lin Lu

*University of Wollongong, ll972@uowmail.edu.au*

Wenxian Li

*University of Wollongong, wenxian@uow.edu.au*

Jung Ho Kim

*University of Wollongong, jhk@uow.edu.au*

*See next page for additional authors*

Follow this and additional works at: <https://ro.uow.edu.au/engpapers>



Part of the [Engineering Commons](#)

<https://ro.uow.edu.au/engpapers/3241>

---

#### Recommended Citation

Zeng, Rong; Dou, S X.; Lu, Lin; Li, Wenxian; Kim, Jung Ho; Munroe, Paul G.; Zheng, Rongkun; and Ringer, S P: Thermal-strain-induced enhancement of electromagnetic properties of SiC-MgB2 composites 2009, 1-3.

<https://ro.uow.edu.au/engpapers/3241>

Research Online is the open access institutional repository for the University of Wollongong. For further information contact the UOW Library: [research-pubs@uow.edu.au](mailto:research-pubs@uow.edu.au)

---

## Authors

Rong Zeng, S X. Dou, Lin Lu, Wenxian Li, Jung Ho Kim, Paul G. Munroe, Rongkun Zheng, and S P. Ringer

## Thermal-strain-induced enhancement of electromagnetic properties of SiC–MgB<sub>2</sub> composites

R. Zeng, S. X. Dou, L. Lu, W. X. Li, J. H. Kim et al.

Citation: *Appl. Phys. Lett.* **94**, 042510 (2009); doi: 10.1063/1.3078396

View online: <http://dx.doi.org/10.1063/1.3078396>

View Table of Contents: <http://apl.aip.org/resource/1/APPLAB/v94/i4>

Published by the American Institute of Physics.

---

### Related Articles

Growth, structure and dielectric characteristics of Ba[(Fe<sub>1</sub>/2Nb<sub>1</sub>/2)0.1Ti0.9]O<sub>3</sub> thin films by pulsed laser deposition

*J. Appl. Phys.* **113**, 044114 (2013)

Evaluation of Sr<sub>2</sub>MMoO<sub>6</sub> (M=Mg, Mn) as anode materials in solid-oxide fuel cells: A neutron diffraction study

*J. Appl. Phys.* **113**, 023511 (2013)

Promotion of [001]-oriented L1<sub>0</sub>-FePt by rapid thermal annealing with light absorption layer

*Appl. Phys. Lett.* **101**, 252403 (2012)

Morphology-influenced thermal conductivity of polyethylene single chains and crystalline fibers

*J. Appl. Phys.* **112**, 094304 (2012)

Tailoring thermal expansion in metal matrix composites blended by antiperovskite manganese nitrides exhibiting giant negative thermal expansion

*J. Appl. Phys.* **112**, 083517 (2012)

---

### Additional information on *Appl. Phys. Lett.*


Journal Homepage: <http://apl.aip.org/>

Journal Information: [http://apl.aip.org/about/about\\_the\\_journal](http://apl.aip.org/about/about_the_journal)

Top downloads: [http://apl.aip.org/features/most\\_downloaded](http://apl.aip.org/features/most_downloaded)

Information for Authors: <http://apl.aip.org/authors>

## ADVERTISEMENT



**JANIS**

**Does your research require low temperatures? Contact Janis today.  
Our engineers will assist you in choosing the best system for your application.**

**10 mK to 800 K Cryocoolers**  
**LHe/LN<sub>2</sub> Cryostats**  
**Dilution Refrigerator Systems**  
**Magnet Systems**  
**Micro-manipulated Probe Stations**

**sales@janis.com    www.janis.com**  
**Click to view our product web page.**

# Thermal-strain-induced enhancement of electromagnetic properties of SiC–MgB<sub>2</sub> composites

R. Zeng,<sup>1</sup> S. X. Dou,<sup>1,a)</sup> L. Lu,<sup>1</sup> W. X. Li,<sup>1</sup> J. H. Kim,<sup>1</sup> P. Munroe,<sup>2</sup> R. K. Zheng,<sup>3</sup> and S. P. Ringer<sup>3</sup>

<sup>1</sup>*Institute for Superconducting and Electronic Materials, University of Wollongong, Northfields Avenue, Wollongong, New South Wales 2522, Australia*

<sup>2</sup>*Electron Microscope Unit, University of New South Wales, Sydney, New South Wales 2052, Australia*

<sup>3</sup>*Electron Microscope Unit, University of Sydney, Sydney, New South Wales 2000, Australia*

(Received 10 October 2008; accepted 14 January 2009; published online 30 January 2009)

The effect of thermal strain caused by the different thermal expansion coefficients ( $\alpha$ ) of the MgB<sub>2</sub> and SiC phases on the electromagnetic properties was studied for SiC–MgB<sub>2</sub> composite, which was made by premixing SiC and B, followed by Mg diffusion and reaction. Thermal strain in the MgB<sub>2</sub> phase was demonstrated with x-ray diffraction, Raman spectroscopy, and transmission electron microscopy. In contrast to the common practice of improving the critical current density  $J_c$  and the upper critical field  $H_{c2}$  of MgB<sub>2</sub> through chemical substitution, by taking advantage of residual thermal strains, we are able to design a composite showing only a small decrease in the critical temperature and a little increase in resistivity but a significant improvement over the  $J_c$  and  $H_{c2}$  of pure MgB<sub>2</sub>. © 2009 American Institute of Physics. [DOI: 10.1063/1.3078396]

Strain engineering has been used to modify the properties of materials in ferroelectric,<sup>1</sup> superconducting,<sup>2</sup> and ferromagnetic thin films.<sup>3</sup> Here, we report the observation of residual thermal stress/strain in dense SiC–MgB<sub>2</sub> superconductor composites prepared by a diffusion method. The doping of nano-SiC particles into MgB<sub>2</sub> has been proven to be particularly effective in significantly enhancing the critical current density  $J_c$ , the irreversibility field  $H_{irr}$ , and the upper critical field  $H_{c2}$ .<sup>4–8</sup> Extensive work has been carried out to understand the mechanism behind the special doping effects of C and SiC.<sup>4,5,9</sup> Recently, a dual reaction model has been proposed to provide a more comprehensive understanding of nano-SiC doping in MgB<sub>2</sub>.<sup>5</sup> The disadvantages of nano-SiC doping are the reduction in the critical temperature  $T_c$  and the increase in resistivity, resulting in the deterioration of low-field  $J_c$ .

In this work, we designed and fabricated a SiC–MgB<sub>2</sub> composite by a diffusion reaction of Mg with a premixed B–SiC bulk. Starting powders of crystalline B (99.999%), with and without 10 wt % SiC particles, were mixed and pressed into pellets. The pellets were then put into an iron tube filled with Mg powder (99.8%). The atomic ratio between Mg and B was 1.15:2.0. Since the formation of MgB<sub>2</sub> was accomplished via a diffusion process, long reaction times were thus needed to obtain a fully reacted MgB<sub>2</sub> bulk. The samples were sintered at 923–1223 K for 10 h in a quartz tube, where a flow of high purity argon gas was maintained, and then furnace-cooled to room temperature. All samples were characterized by x-ray diffraction (XRD) and analyzed using Rietveld refinement. Microstructural observations were performed by using scanning electron microscopy (SEM), field emission SEM, and transmission electron microscopy (TEM). The magnetization of samples was measured at 5 and 20 K using a quantum design physical properties measurement system. The irreversibility field  $H_{irr}$  and

$H_{c2}$  could be deduced using the criteria of 0.1 and 0.9 of  $\rho(H, T)$ , respectively.

The  $a$ - and  $c$ -axis lattice parameters and the SiC content were determined as shown in Table I. We note that the  $a$ -axis parameter is virtually the same for both the doped and undoped samples, while the  $c$ -axis parameter is slightly enlarged in the SiC–MgB<sub>2</sub> composite. In contrast, the  $a$ -axis parameter for *in situ* processed SiC doped MgB<sub>2</sub> is reduced, while the  $c$ -axis parameter generally remains unchanged, as reported by a number of groups.<sup>4,5</sup> It is also interesting to note that the SiC particles remained unreacted and formed a composite with the MgB<sub>2</sub> in the SiC-doped sample. The Rietveld refinement analysis results showed that there was about 9.3 wt % SiC, which is about the same as in the starting precursor. This result may be due to both the crystalline, rather than amorphous, nature of the SiC and the diffusion process and is consistent with the fact that the XRD patterns showed no presence of Mg<sub>2</sub>Si, in clear contrast to SiC-doped MgB<sub>2</sub> prepared by the *in situ* technique.<sup>4,5</sup> Mg<sub>2</sub>Si is always present in such *in situ* samples due to the reaction of Mg with SiC. The reason why the SiC additives did not decompose and react with the Mg is largely attributed to the fact that crystalline SiC was used, which is not as reactive as amorphous SiC, as has been reported previously. Crystalline SiC has been used as a substrate material, and it showed complete compatibility with MgB<sub>2</sub> films with no evidence of any reaction.<sup>9</sup>

There is a small drop (0.6 K) in  $T_c$  and a small increase in  $\rho(40\text{ K})$  (from 12 to 16  $\mu\Omega\text{ cm}$ ) for the SiC-doped sample. In contrast, *in situ* processed SiC doped MgB<sub>2</sub> normally experiences a decrease in  $T_c$  from 1.5 to 2 K (Ref. 9) and an increase in  $\rho(40\text{ K})$  from 90 to 300  $\mu\Omega\text{ cm}$ .<sup>5</sup> These SiC–MgB<sub>2</sub> composite samples had a high  $T_c$  value (37.8 K) and low  $\rho(40\text{ K})$  (Table I). It is interesting to note that the SiC–MgB<sub>2</sub> composite sample showed not only an improved in-field  $J_c$  but also a lack of degradation and even an enhancement in the self-field  $J_c$ , as shown in Fig. 1(a) and Table I, while it has been well established that nano-SiC doping using the conventional *in situ* technique reduces the

<sup>a)</sup> Author to whom correspondence should be addressed. Electronic mail: shi@uow.edu.au.

TABLE I. Summary of physical properties of pure and SiC–MgB<sub>2</sub> composite samples.

Sample	Density (g/cm <sup>3</sup> )	<i>a</i> - and <i>c</i> -axis parameters (Å)	Defect induced nonuniform lattice strain (XRD)		Mg vacancies XRD (%)	Grain size TEM (nm)	<i>T<sub>c</sub></i> (K)	$\rho(40\text{ K})$ ( $\mu\Omega\text{ cm}$ )
			<i>a</i> -axis (%)	<i>c</i> -axis (%)				
Pure	1.86	3.085 and 3.5230	0.208	0.292	3.2	~100	38.4	12
10% SiC	1.91	3.084 and 3.5282	0.306	1.13	3.6	~100	37.8	16

self-field  $J_c$ .<sup>1</sup> The  $H_{irr}$  and  $H_{c2}$  of the SiC–MgB<sub>2</sub> sample are significantly improved in comparison with the pure sample, as shown in Fig. 1(b).

The above results raise a serious question concerning the nature of the mechanism behind the significant property enhancement in SiC–MgB<sub>2</sub> composite, as these effects cannot be explained by the dual reaction model<sup>4</sup> or C substitution.<sup>4,5</sup> Because the residual SiC is the dominating impurity, this enabled us to isolate the special effects of residual SiC. As the difference in the thermal expansion coefficients ( $\alpha$ ) between SiC and MgB<sub>2</sub> is quite large, which can create thermal strains in the MgB<sub>2</sub> matrix during cooling, we can examine whether the residual thermal strain could be an effective pinning mechanism.

The difference in  $\alpha$  between MgB<sub>2</sub> and SiC dictates the stress status of the MgB<sub>2</sub> and causes thermal strain in the MgB<sub>2</sub> matrix around the SiC particles during the cooling process. The lattice changes and lattice strain in the MgB<sub>2</sub> matrix during cooling can be derived from the  $\alpha$  data.<sup>10,11</sup> If the two phases are strongly bonded, the MgB<sub>2</sub> phase will be subjected to a tensile strain on cooling. In particular, there will be a larger strain along the *c*-axis since there is a larger difference in  $\alpha$  along the *c*-axis between MgB<sub>2</sub> and SiC. Our calculation indicated that the lattice strain is as large as  $-0.55\%$  in the MgB<sub>2</sub> along the *c*-axis at room temperature. This value is approximately equal to the critical strain rate measured for multifilament MgB<sub>2</sub> wires,<sup>12</sup> which showed that the  $J_c$  increased with increasing tensile strain rate, although this strain was measured on the macroscale. The increased strain in the SiC–MgB<sub>2</sub> is also evident from the larger full width at half maximum (FWHM) values [ $0.48^\circ$  for the (002) peak] than for pure MgB<sub>2</sub> [ $0.326^\circ$  for the (002) peak]. The increase in the FWHM can be solely attributed to the increase in the strain since the grain sizes of both samples

are the same. Using Williamson–Hall analysis, we calculated the lattice strain to be 0.208% and 0.306% along the *a*-axis and 0.292% and 1.13% along the *c*-axis for the pure and SiC–MgB<sub>2</sub> samples, respectively (Table I).

The thermal strain could create a huge stress field, structural defects, and lattice distortion in the MgB<sub>2</sub> matrix, which would remain in the SiC–MgB<sub>2</sub> sample during cooling. TEM examination revealed the following features. (1) SiC and MgB<sub>2</sub> remain as separate phases and form a strongly bonded composite, as shown in Figs. 2(a) and 2(b). The SiC particles, while micron sized in scale, are comprised of smaller grains a few nanometers in size. It is these small grains that assist in providing excellent wetting and contact with the MgB<sub>2</sub> phase. (2) The grain size for both pure MgB<sub>2</sub> and MgB<sub>2</sub> in the SiC–MgB<sub>2</sub> composite is the same ( $\sim 100$  nm). (3) There is a high density of defects (dislocations and lattice distortion) in the MgB<sub>2</sub> phase along the interfaces between the SiC and MgB<sub>2</sub>, as indicated by the arrows in Fig. 2(a), which may be attributable to the tensile strain in the MgB<sub>2</sub> phase that is imposed by the small thermal expansion of SiC during cooling. Figure 2(b) shows the interface between the two coexisting phases of MgB<sub>2</sub> and SiC. The electron diffraction patterns taken from both sides indicate that the two phases are faceted with the [101] plane of SiC and the [001] plane of MgB<sub>2</sub>. The thermal expansion coefficient for MgB<sub>2</sub> is highly anisotropic with a large variation in the [001] direction, while that for SiC is nearly isotropic. Thus, this kind of interface will impose tensile stress along the *c*-axis in MgB<sub>2</sub>. In comparison, these wave structures are hardly seen in the pure MgB<sub>2</sub> sample. Careful examination indicated that these fringes were induced by lattice mismatch between two layers, so dislocations and lattice distortions were commonly observed in the areas showing the fringes. The lattice distortion observed in TEM confirmed

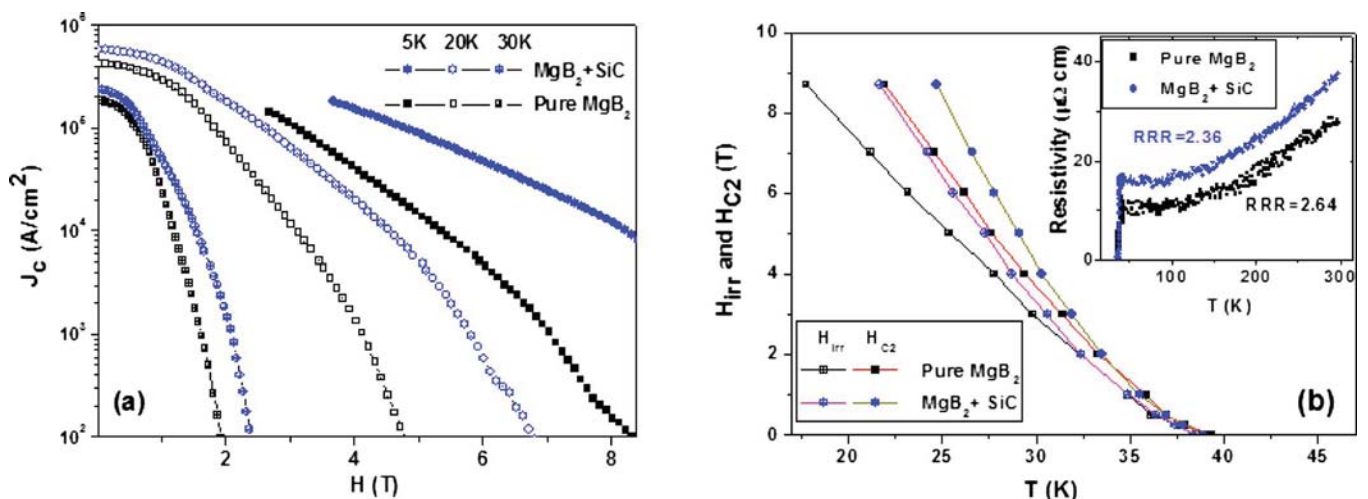


FIG. 1. (Color online) (a) The magnetic  $J_c$  vs field at 5 and 20 K for the pure and the nano-SiC doped samples and (b) upper critical field ( $H_{c2}$ ) and irreversibility field ( $H_{irr}$ ) as functions of the temperature. The inset shows the resistivity of these samples as a function of temperature.



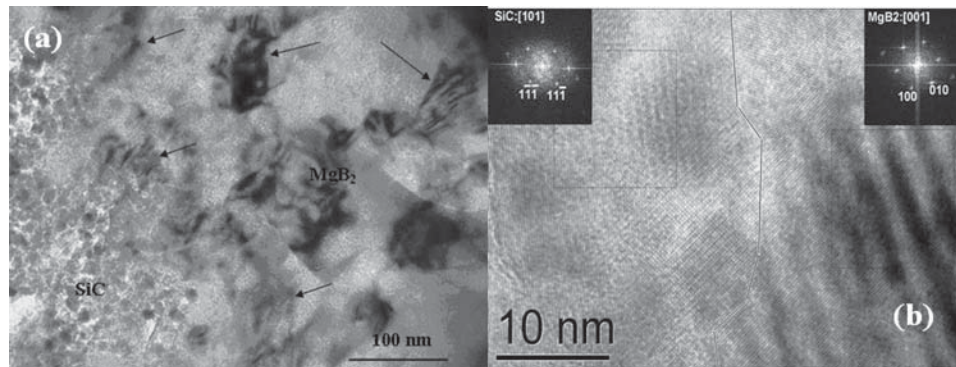


FIG. 2. Bright field TEM images of the two-phase composite and defects along the boundaries between the SiC particles and the MgB<sub>2</sub> matrix. Defects are indicated by arrows, and magnification is indicated by the length of the respective scale bar, which is (a) 100 nm, (b) 10 nm. (b) shows a high resolution TEM image of the interface with inset electron diffraction patterns of SiC and MgB<sub>2</sub> from each side of the interface. The middle line shows the actual interface of SiC and MgB<sub>2</sub>, which indicates the strong bonding of MgB<sub>2</sub> with SiC.

our Raman measurement results, which are described below.

Raman spectroscopy is known to be an excellent probe for the detection and estimation of these stresses and strains or lattice distortions. The peaks centered at the phonon density of states (PDOS) are understood to arise due to disorder and distortion.<sup>13</sup> A compressive stress is indicated by a shift of the Raman peak to higher frequencies, while a tensile stress is indicated by a shift of the Raman peak to lower frequencies.<sup>14</sup> The relative intensity and FWHM of the PDOS peaks reflect the extent of the distortion.<sup>15</sup> Figure 3 shows the normalized ambient Raman spectra of the samples sintered at 1123 K for 10 h. The  $E_{2g}$  and PDOS peaks are shifted to lower frequency for the SiC-doped sample ( $E_{2g}$ :576 cm<sup>-1</sup>, PDOS:762 cm<sup>-1</sup>) compared with the pure sample ( $E_{2g}$ :600 cm<sup>-1</sup>, PDOS:770 cm<sup>-1</sup>), which indicates that there is residual tensile strain in the original SiC-MgB<sub>2</sub> composite sample. By comparing the Raman spectra of samples before and after cooling to low temperature (down to 10 K), we find that the most obvious changes in the Raman peaks are that the shifting tendency of the two main Raman peaks, the FWHM of both peaks, and the intensity of the main PDOS peak are increased by the cooling process for the SiC-doped sample but not changed for the pure sample.

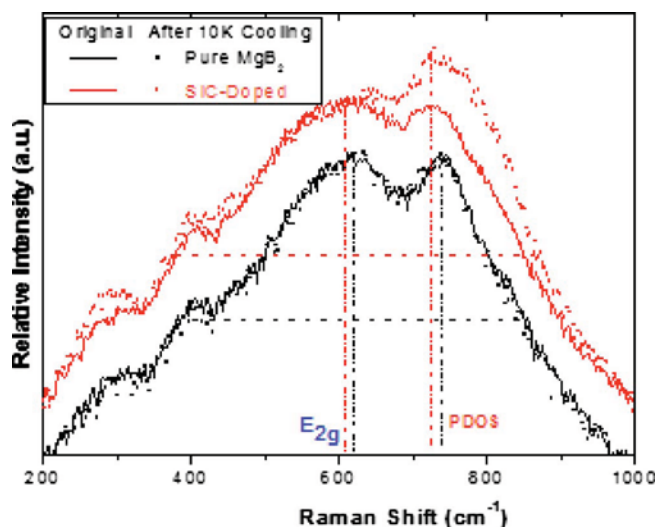


FIG. 3. (Color online) The normalized ambient Raman spectra of samples sintered at 850 °C for 10 h. The line spectra correspond to measurements taken before, and the dot spectra to measurements taken after cooling to 10 K for pure MgB<sub>2</sub> (black) and SiC+MgB<sub>2</sub> (red) composite.

The enhanced PDOS peak in the SiC-doped sample is an indication of the increased residual strain, which leads to enhanced flux pinning and thus improves the  $J_c$  and  $H_{c2}$ .

The present findings have a significant implication, as they open up a new direction for numerous bulk composites that can be strain-engineered to achieve desirable material properties without significant alteration in intrinsic properties, as compared to chemical substitution.

The authors thank Professor R. Flükiger, Professor E. W. Collings, and Dr. T. Silver for their help and useful discussions. This work is supported by the Australian Research Council (Project No. DP0770205), Hyper Tech Research Inc.

- <sup>1</sup>K. J. Choi, M. Biegalski, Y. L. Li, A. Sharan, J. Schubert, R. Uecker, P. Reiche, Y. B. Chen, X. Q. Pan, V. Gopalan, L. Q. Chen, D. G. Schlom, and C. B. Eom, *Science* **306**, 1005 (2004).
- <sup>2</sup>I. Bozovic, G. Logvenov, I. Belca, B. Narimbetov, and I. Sveklo, *Phys. Rev. Lett.* **89**, 107001 (2002).
- <sup>3</sup>S. K. Streiffer, J. A. Eastman, D. D. Fong, C. Thompson, A. Munkholm, M. V. R. Murty, O. Auciello, G. R. Bai, and G. B. Stephenson, *Phys. Rev. Lett.* **89**, 067601 (2002).
- <sup>4</sup>S. X. Dou, O. Shcherbakova, W. K. Yoeh, J. H. Kim, S. Soltanian, X. L. Wang, C. Senatore, R. Flukiger, M. Dhallo, O. Husnjak, and E. Babic, *Phys. Rev. Lett.* **98**, 097002 (2007).
- <sup>5</sup>A. Matsumoto, H. Kumakura, H. Kitaguchi, B. J. Senkowicz, M. C. Jewell, E. E. Hellstrom, Y. Zhu, P. M. Voyles, and D. C. Larbalestier, *Appl. Phys. Lett.* **89**, 132508 (2006).
- <sup>6</sup>M. D. Sumption, M. Bhatia, M. Rindfleisch, M. Tomsic, S. Soltanian, S. X. Dou, and E. W. Collings, *Appl. Phys. Lett.* **86**, 092507 (2005).
- <sup>7</sup>Y. Zhu, A. Matsumoto, B. J. Senkowicz, H. Kumakura, H. Kitaguchi, M. C. Jewell, E. E. Hellstrom, D. C. Larbalestier, and P. M. Voyles, *J. Appl. Phys.* **102**, 013913 (2007).
- <sup>8</sup>K. Togano, T. Nakane, H. Fujii, H. Takeya, and H. Kumakura, *Supercond. Sci. Technol.* **19**, L17 (2006).
- <sup>9</sup>X. H. Zeng, A. V. Pogrebnyakov, M. H. Zhu, J. E. Jones, X. X. Xi, S. Y. Xu, E. Wertz, Q. Li, J. M. Redwing, J. Lettieri, V. Vaithyanathan, D. G. Schlom, Z. K. Liu, O. Trithaveesak, and J. Schubert, *Appl. Phys. Lett.* **82**, 2097 (2003).
- <sup>10</sup>J. J. Neumeier, T. Tomita, M. Debessai, J. S. Schilling, P. W. Barnes, D. G. Hinks, J. D. Jorgensen, *Phys. Rev. B* **72**, 220505 (2005).
- <sup>11</sup>J. D. Jorgensen, D. G. Hinks, and S. Short, *Phys. Rev. B* **63**, 224522 (2001).
- <sup>12</sup>M. Dhallo, H. van Weeren, S. Wessel, A. den Ouden, H. H. J. ten Kate, I. Husek, P. Kovac, S. Schlachter, and W. Goldacker, *Supercond. Sci. Technol.* **18**, S253 (2005).
- <sup>13</sup>K. P. Bohnen, R. Heid, and B. Renker, *Phys. Rev. Lett.* **86**, 5771 (2001).
- <sup>14</sup>V. Paillard, P. Puech, R. Sirvin, S. Hamma, and P. R. I. Cabarrocas, *J. Appl. Phys.* **90**, 3276 (2001).
- <sup>15</sup>W. X. Li, Y. Li, R. H. Chen, R. Zeng, S. X. Dou, M. Y. Zhu, and H. M. Jin, *Phys. Rev. B* **77**, 094517 (2008).